IJC Heart & Vessels 3 (2014) 68–74

Contents lists available at ScienceDirect

IJC Heart & Vessels

journal homepage: http://www.journals.elsevier.com/ijc-heart-and-vessels

Optical coherence tomography characteristics of in-stent restenosis are different between first and second generation drug eluting stents ☆

Kadriye Kilickesmez [a,*,1], Gianni Dall'Ara [a,1], Juan Carlos Rama-Merchan [a], Matteo Ghione [a], Alessio Mattesini [a], Carlos Moreno Vinues [a], Nikolaos Konstantinidis [a], Michele Pighi [a], Rodrigo Estevez-Loureiro [a], Carlo Zivelonghi [a], Alistair C. Lindsay [a], Gioel G. Secco [a,b], Nicolas Foin [c], Ranil De Silva [a,c], Carlo Di Mario [a,c]

[a] NIHR Biomedical Research Unit, Royal Brompton Hospital & Harefield NHS Foundation Trust, London, UK
[b] Department of Clinical and Experimental Medicine, University of Eastern Piedmont, Novara, Italy
[c] National Heart and Lung Institute, Imperial College London, London, UK

ARTICLE INFO

Article history:
Received 15 February 2014
Accepted 10 March 2014
Available online 19 March 2014

Keywords:
Optical coherence tomography
In-stent restenosis
Drug eluting stent
Neoatherosclerosis

ABSTRACT

Aims: Characterization of neointimal tissue is essential to understand the pathophysiology of in-stent restenosis (ISR) after drug eluting stent (DES) implantation. Using optical coherence tomography (OCT), we compared the morphologic characteristics of ISR between first and second generation DES.

Methods and Results: OCT was performed in 66 DES-ISR, defined as >50% angiographic diameter stenosis within the stented segment. Patients with ISR of first generation sirolimus-eluting stents (SES), paclitaxel eluting stents (PES) and second generation zotarolimus-eluting stents (ZES), everolimus-eluting stents (EES) and biolimus-eluting stents (BES) were enrolled. Quantitative and qualitative ISR tissue analysis was performed at 1-mm intervals along the entire stent, and categorised as homogeneous, heterogeneous and neo-atherosclerosis. The presence of microvessels and peri-strut low intensity area (PSLIA) was determined in all ISR. Neoatherosclerosis was identified by lipid, calcium and thin-cap fibro-atheroma (TCFA) like lesions. We compared the two DES generations at both early (<1 year) and late (>1 year) follow-ups.

In second generation DES a heterogeneous pattern was prevalent both before and after 1 year (57.1% and 58.6% respectively). Neo-atherosclerosis was more common in the early period in first generation DES (19.4% vs 11.7%, $p < 0.01$), but after one year was more prevalent in second generation DES (7.0% vs 19.3%, $p < 0.01$). Similar prevalence of TCFAs was observed in both groups in all comparisons.

Conclusions: When ISR restenosis occurs in second generation DES, the current data suggest a different time course and different morphological characteristics from first generation. Future prospective studies should evaluate the relationship between ISR morphology, time course and clinical events.

1. Introduction

Although a significant reduction in the rate of in-stent restenosis (ISR) has been observed with first and second generation (G1 and G2) drug eluting stents (DES) compared with bare metal stents (BMS), this event still limits long term outcomes after percutaneous coronary intervention (PCI) (1,2). However, the basis for this observation is not yet fully understood. Optical coherence tomography (OCT) is the preferred modality to study arterial healing after stent implantation. Due to its high resolution, OCT can disclose plaque morphology with a sensitivity close to histology and provide an accurate assessment of stent deployment, with special focus on the number and distribution of covered struts (3,4). Recently, OCT has been used for the characterization of ISR and different tissue patterns have been described (5,6). Studies of DES-ISR are limited but there is an evidence that neointimal hyperplasia after DES may be more heterogeneous and occur earlier than the fibrotic intimal hyperplasia observed after BMS implantation (7,8). Furthermore, there is a histological evidence of neoatherosclerotic tissue growth, mainly described within first generation DES-ISR, which is characterized by lipid and/or calcium deposition, macrophage infiltration and necrotic core formation. In some cases these lesions are almost indistinguishable from thin-cap-fibro-atheroma (TCFA) lesions found in native plaques (8,9) which are consistently shown to correlate with

☆ Relationship with industries: Nothing to disclose.

* Corresponding author at: Royal Brompton Hospital, Sydney Street, London SW3 6NP, UK. Tel./fax: +44 207351.
E-mail address: kadriye11@yahoo.com (K. Kilickesmez).

[1] These two authors contributed equally to the manuscript.

http://dx.doi.org/10.1016/j.ijchv.2014.03.003

acute coronary events (10–12). G2 DES, probably because of greater biocompatibility, have drastically reduced restenosis and stent thrombosis when compared with G1 DES (13–16). However, ISR has also been described with these new generation devices.

The aim of this study was to compare the morphologic characteristics of neo-intimal tissue in a consecutive series of ISR of G1 and G2 DES studied with OCT.

2. Methods

2.1. Study design and population

All consecutive patients with one or more ISR in a G1 or G2 DES, studied with OCT between January 2007 and December 2012, were considered for the study. ISR was defined as angiographically documented diameter stenosis greater than 50% within the stented segment. The region of interest extended from the distal to the proximal stent edge, excluding the margins. As in previous pathologic ISR studies (8), we considered overlapping and consecutive stents as one lesion, while stents separated by more than 5 mm were considered as separate lesions. Patients included in our study underwent coronary angiography as clinically indicated, due to stable angina or NSTE-acute coronary syndromes, or as elective scheduled angiographic follow-up (because of the type of lesion previously treated [left main or equivalent] or as part of approved DES trials) (17,18). The use of intravascular imaging with IVUS or OCT is routinely practised in our centre to diversify the treatment of ISR based on its prevalent mechanism (underexpansion vs hyperproliferation) as indicated and explained in the informed consent approved by the institutional review board. We excluded patients with total occlusion, ST-segment elevation myocardial infarction, cardiogenic shock, serum creatinine >2 mg/dl and bare metal stent ISR.

2.2. Quantitative coronary angiography

Quantitative coronary angiography (QCA) was performed offline by a skilled analyzer blinded to patients' clinical characteristics and OCT analysis, using dedicated cardiovascular measurement software (QAngio XA 7.1 Medis Medical Imaging System, Leiden, The Netherlands) on a single, selected 2D end-diastolic image frame. Care was taken to select projections and frames with minimal foreshortening and vessel overlap, analyzing the view that revealed the highest degree of stenosis. After careful calibration, lesion length, proximal and distal references, minimal luminal diameter (MLD) and percent diameter stenosis (%DS) were calculated. Based on QCA results, lesions were classified as focal restenosis: <10 mm in length, or diffuse restenosis: >10 mm in length (19).

2.3. Optical coherence tomography imaging and analysis

The OCT images were acquired, using a non-occlusive technique, through a 2.7 Fr C7 Dragonfly Imaging Catheter (LightLab Imaging Inc., Westford, MA, USA), flushed with undiluted contrast dye and calibrated before the acquisition, which was inserted distal to the lesion of interest. A mechanical pullback at a speed of 20 mm/s was started during continuous automatic flushing of 2–5 ml/s of iodixanol (Visipaque™ 320 mg I/ml GE Healthcare, Amersham, UK) to ensure blood clearance from the coronary arteries, using a Medrad injector (Medrad Inc., Warrendale, PA, USA).

Quantitative and qualitative OCT analyses were performed off-line by agreement of two experienced analysts, blinded to clinical and angiographic lesion characteristics using commercial software (LightLab; St. Jude, Minneapolis, MN, USA), at every 1 mm cross section (CS) throughout the pullback from the distal to the proximal stent edge. Quantitative measurements included lumen and stent cross-sectional areas (CSA) (automatically traced and manually adjusted when required), neointimal hyperplasia (NIH) area (stent area–lumen area), percentage of NIH area (NIH area / stent area × 100) (Fig. 1) (20). For this analysis, only CSs with a percentage of NIH area ≥50% have been considered as effective part of the restenotic segment within stent (20).

Owing to a lack of consensus regarding the classification of ISR optical patterns and their histopathological basis, we analysed every evaluable cross section and adopted previously reported qualitative criteria for this analysis (6,9) (Fig. 2): 1) *homogeneous neointima*; 2) *heterogeneous neointima*; and 3) *neo-atherosclerosis*. The homogeneous pattern consists of tissue with uniform optical properties and no focal variation in backscattering. Heterogeneous tissue was identified by the presence of several variations in the optical backscattering properties and sub-classified in: *layered pattern*, consisting in concentric layers with different optical properties (thick adluminal high scattering layer and an abluminal low scattering layer), *patchy pattern*, irregular and highly echo-lucent regions throughout the layers, and *speckled pattern*, restenotic tissue with heterogeneous speckled bands (6,21). We defined neo-atherosclerosis as ISR showing optical areas consistent with at least one of the following features: *lipids*, diffusely bordered, signal-poor regions; *calcium* as well-delineated, low back-scattering heterogeneous regions; and *thin-cap fibro-atheroma* (TCFA) plaques, with a fibrous cap thickness ≤65 μm and an angle of lipid tissue ≥180 showing relevant signal attenuation (3,22). In these neo-atherosclerotic lesions, we also identified the presence of *macrophages*, multiple strong back reflections, resulting in a relatively high OCT signal variance within the fibrous cap (23). Hence, in the presence of the well defined neo-atherosclerotic features reported above, we classified the ISR as *neo-atherosclerosis*, while we defined the *heterogeneous* group as those with an ISR optical pattern which was neither homogeneous nor neoatherosclerotic tissue.

Furthermore, in all lesions we identified the presence of: *microvessels*, low backscattering structure with a diameter <200 μm; *peri-strut low intensity area* (PSLIA) defined as a region around stent struts with homogeneous lower intensity than surrounding tissue, without signal attenuation (24); *malapposed struts*, when the axial distance from DES strut to the luminal surface was longer than the strut/polymer thickness (25), excluding bifurcations; and *uncovered struts*, NIH thickness equal to 0 μm (26).

The decision to perform a dilatation before proceeding to OCT acquisition was left to the operator's discretion on the basis of the angiographic findings. In the event of a tight ISR lesion, pre-dilation with a 2.0 semi-compliant balloon, inflated at nominal pressure was allowed. Since balloon inflation may create a rupture of the fibrous cap, we excluded from our analysis disrupted intima like lesions and the presence of intraluminal material.

2.4. Statistical analysis

Categorical variables are expressed as numbers (percentages) and comparisons between groups were performed with χ^2 or Fisher's exact test. Continuous variables are expressed as the mean ± standard deviation and compared with Independent T-test. The primary analysis compared ISR characteristics at early follow-up (less than 1 year) and late follow-up (more than 1 year) within the first or the second generation groups. Next, the comparison was performed between generations, within the early or late period (20). A p value <0.05 was considered statistically significant. All statistical analyses were performed using the SPSS software (SPSS Inc. Version 20, Chicago, Illinois).

2.5. Results

A total of 66 ISR lesions were identified in 41 consecutive patients enrolled in this study. We found 44 ISR within G1 DES: 21 sirolimus-eluting stents (SES) (Cypher SELECT, Cordis, Miami Lakes, FL, USA) and 23 paclitaxel-eluting stents (PES) (Taxus EXPRESS and Liberté, Boston Scientific, Natick, MA, USA). We also identified 22 ISR lesions in G2 DES: of which 11 everolimus-eluting stents (EES) (9 Xience, Abbott Vascular, Santa Clara, CA, USA; and 2 Promus, Boston Scientific,

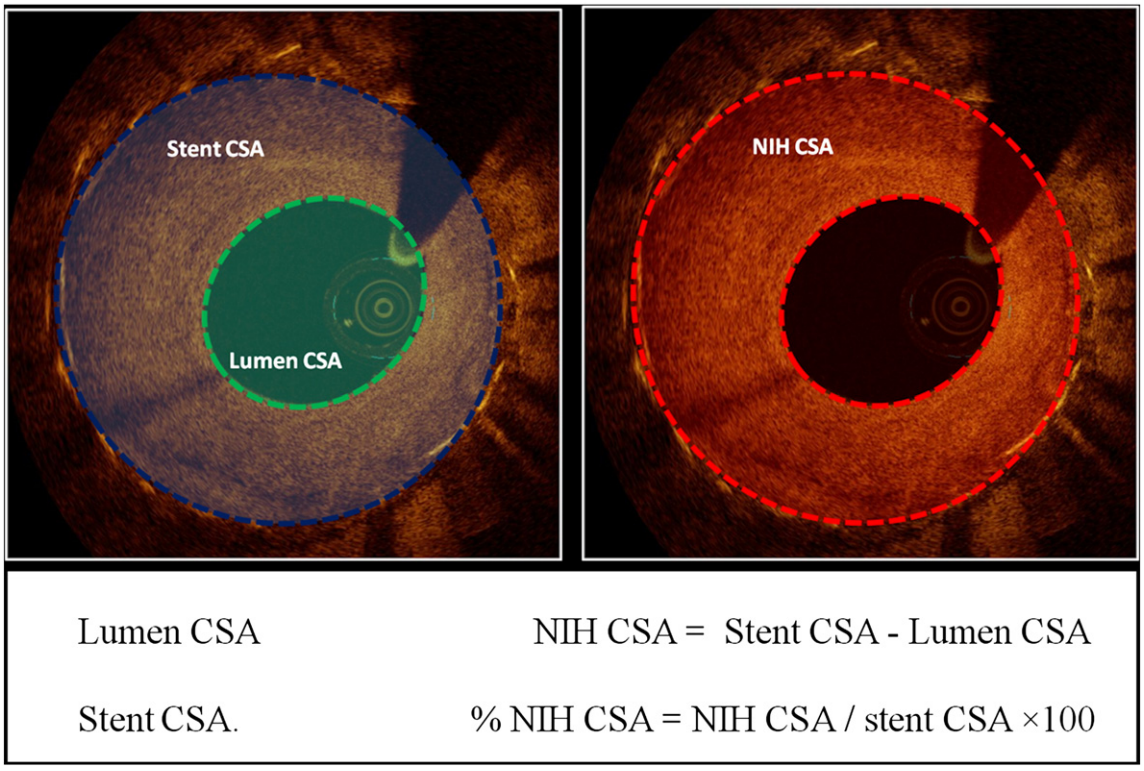

Fig. 1. Quantitative optical coherence tomography analysis. Representation of measured areas. CSA: cross sectional area; NIH: neointimal hyperplasia.

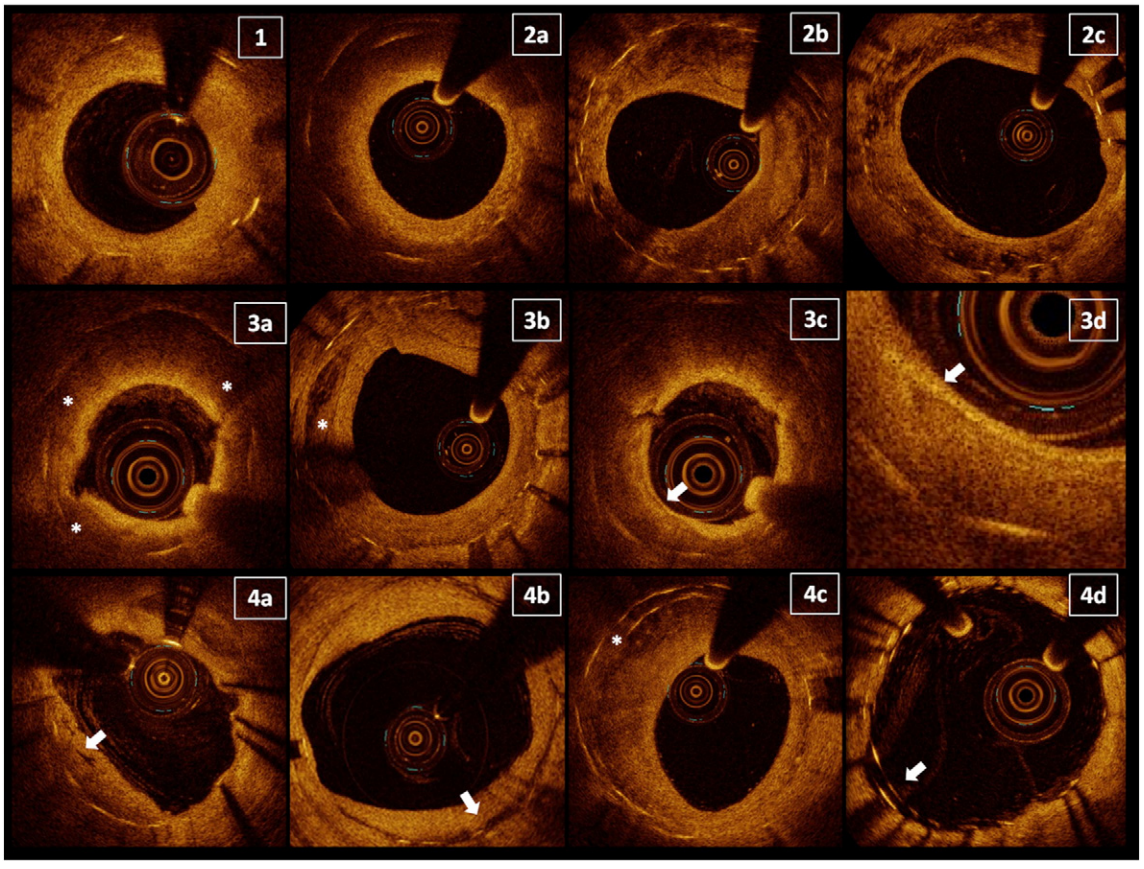

Fig. 2. Qualitative optical coherence tomography analysis. For definitions, refer in the text. 1) Homogeneous pattern of ISR. 2) Heterogeneous patterns subsequently subdivided in three subtypes: 2a) layered pattern; 2b) patchy pattern; and 2c) speckled pattern. 3) Neo-atherosclerosis and its main features: 3a) lipid plaque; 3b) calcium deposit; 3c) thin-cap fibroatheroma; and 3d) detail of macrophage presence in a lipid plaque. 4) Miscellaneous ISR characteristics: 4a) microvessels; 4b) peri-strut low intensity areas; 4c) overlapping stents; and 4d) malapposed struts.

Natick, MA, USA) 10 zotarolimus-eluting stents (ZES) (Resolute, Medtronic, Santa Rosa, CA, USA) and 1 biolimus-eluting stent (BES) (BioMatrix Flex, Biosensors Inc, Newport Beach, CA, USA) (Fig. 3). Coronary angiography was clinically driven in 58.2% of cases and electively scheduled in the remaining. Only 5 lesions (7.6%) required balloon pre-dilatation before OCT pullback.

2.6. Clinical characteristic

Baseline patients' clinical characteristics are shown in Table 1. There were no major differences between groups with the exception of a higher prevalence of previous myocardial infarction within G2 group in those with longer follow-up compared with patients with shorter follow-up ($p = 0.04$). More often the left circumflex was the culprit artery in the early follow-up of G1 compared with G2 DES ($p = 0.04$). The rate of use of ACE-inhibitors differed among groups.

2.7. QCA analysis

QCA analyses are summarised in Table 2. Within G1 DES focal restenosis predominated, whereas in G2 ISR a diffused pattern was prevalent before 1 year with focal ISR more frequent at later time points ($p = 0.02$).

Quantitative analyses did not differ between early and late ISR of G1 DES. In the G2 group, the earlier lesions were significantly longer and with lower mean MLD and MLA, as well as higher %DS ($p < 0.01$).

The stent types within each DES generation were similar. Time from stent implantation to the index coronary angiography was not different within the early phase between groups of DES, while in the late comparison it was significantly longer for G1 than G2 DES (37.0 vs 15.8 months, respectively, $p < 0.01$).

2.8. OCT analysis

The quantitative analysis showed similar lesion length among groups. We found different mean absolute values of stent CSA and NIH CSA between generations and that the percentage of NIH CSA was lower for G2 DES both in the early and the late period ($p < 0.01$) (Table 3).

The qualitative analysis performed in the entire stent is reported in Table 4 and Fig. 4. A homogeneous pattern predominated in both early and late G1 DES-ISR, increasing overtime, while the heterogeneous and neoatherosclerotic lesions were less prevalent in the early phase and became even more infrequent at later time points ($p < 0.01$ in all comparisons). In G2 DES, we found a heterogeneous pattern more frequently at both early and late time points. The homogeneous pattern tended to become less prevalent overtime, while the frequency of neoatherosclerotic lesions tended to increase ($p < 0.01$ in all comparisons).

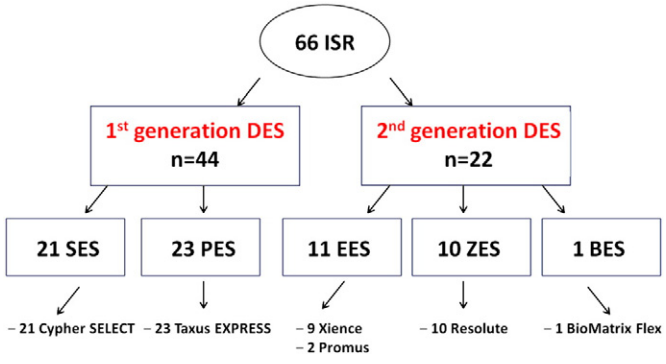

Fig. 3. Schematic view of enrolled stents, according to generation, eluted drug and brand. For acronyms see "Results" chapter.

TCFAs as well as macrophages were rare and their prevalence did not differ between generations and overtime. Microvessels were more common in the early period in G1 ISR, but then decreased in prevalence; PSLIA was less common in G1 but more prevalent in G2 DES ($p < 0.01$). We found similar prevalence of overlapping and malapposed CSs in our analysis, however a significant increase in the number of uncovered struts was found associated with G1 ISR overtime.

3. Discussion

ISR is still the main reason of PCI failure and its predictors seem to be largely the same across the spectrum of BMS, G1 and G2 DES (27). Despite shared trigger factors, several data suggest a different composition of the restenotic tissue within different devices (7–9). Our study, focusing on the evaluation of vascular healing after stent deployment using quantitative and qualitative OCT assessment, depicts a different pattern of ISR between G1 and G2 DES. We compared the two generations at two separate time points, before and after 1 year. Furthermore we analysed the differences of ISR pattern within each generation overtime.

3.1. Comparison between first and second generation DES

We showed that ISR in G1 DES had mainly a homogeneous OCT pattern before and after one year, whereas in G2 DES the heterogeneous features were prevalent. In both generations the percentage of CSs with neo-atherosclerosis remained below 20% and the absolute prevalence was similar between generations. Similar prevalence of TCFAs appeared between generations.

ISR is thought to be a manifestation of abnormal vessel healing after stenting and provides the anatomic substrate for target lesion revascularization (TLR) and possibly acute coronary syndromes (7,28). Although there are few data on the histopathological basis of OCT-ISR patterns, the homogeneous type is thought to be the more common expression of the uncontrolled neointimal cell proliferation typical of BMS. The heterogeneous pattern, sometimes resembling neoatherosclerotic lesions, seems to be more frequent in later phases and in DES (22). Differences in the type of restenosis observed in different DES types have been previously reported (7–9). The underlying processes are likely multifactorial though the precise mechanisms remain unknown. Experimental evidence suggests that neo-atherosclerosis is associated with delayed arterial healing compounded by lethal injury to smooth muscle and endothelial cells (29). Therefore, the heterogeneous OCT images in DES may represent phenomena such as peri-strut inflammation. DES structure itself can influence vessel healing. Variables like different stent platforms, strut thickness, durability of the polymer, kinetics of drug release as well as post-deployment optimisation can explain differences observed in ISR observed in different DES platforms.

There is no consensus on the interpretation of different optical patterns and its histopathological basis. Previous studies demonstrated that restenotic tissue with speckled pattern exhibited myxomatous neointima tissue, containing extracellular matrix with proteoglycans (30,31). DES suppress the immunological response of the treated arterial wall. Therefore, delayed arterial healing, including replacement of extracellular matrix by smooth muscle cells or collagen, might contribute to this speckled image. The layered pattern may arise from a difference in smooth muscle cell density and orientation along the radial axis of ISR, with a more compact and concentric orientation in the inner luminal border, with reduced density and longitudinal orientation toward the vessel exterior. Alternatively the findings may be explained by the progressive attenuation of light travelling through the tissue (6). Conversely, neo-atherosclerosis, as reported in the "methods", is recognized according to well defined OCT features.

Many clinical studies have shown that G2 DES have superior efficacy and safety profile than G1 DES (13–15,17). We need to emphasize that the relationship between ISR morphology determined by OCT and clinical outcome is not established. In this study, only angiographically

Table 1
Baseline clinical characteristics, analysis per patients.

Variable	First generation (n = 30)		p	Second generation (n = 11)		p	p*	p**
	≤1 year (n = 9)	>1 year (n = 21)		≤1 year (n = 7)	>1 year (n = 4)			
Males	8 (88.9)	18 (85.7)	0.81	6 (85.7)	4 (100.0)	0.43	0.85	0.42
Age, years	63.9 ± 7.1	69.7 ± 8.7	0.09	67.9 ± 17.3	61.7 ± 7.4	0.52	0.54	0.10
Diabetes	3 (33.3)	7 (33.3)	NA	5 (71.4)	1 (25.0)	0.14	0.13	0.74
Hypertension	7 (77.8)	17 (81.0)	0.84	6 (85.7)	3 (75.0)	0.66	0.69	0.79
High cholesterol	9 (100.0)	18 (85.7)	0.23	7 (100.0)	4 (100.0)	NA	NA	0.42
History of CAD	6 (66.7)	11 (52.4)	0.69	4 (57.1)	3 (75.0)	0.55	0.70	0.40
Current smoker	3 (33.3)	8 (38.1)	0.80	4 (57.1)	2 (50.0)	0.82	0.34	0.66
Previous CABG	3 (33.3)	10 (47.6)	0.69	5 (71.4)	1 (50.0)	0.48	0.13	0.93
Previous MI	6 (75.0)	14 (73.7)	0.94	2 (33.3)	4 (100.0)	0.04	0.12	0.25
Indication to PCI								
Stable angina	3 (33.3)	11 (52.4)	0.34	4 (57.1)	2 (50.0)	0.82	0.34	0.93
ACS	0 (0.0)	4 (19.0)	0.16	0 (0.0)	0 (0.0)	NA	NA	0.34
Planned follow-up	6 (66.7)	6 (28.6)	0.10	3 (42.9)	2 (50.0)	0.82	0.34	0.40
Vessel with ISR	0 (0.0)	1 (4.8)	0.51	0 (0.0)	0 (0.0)	NA	NA	0.65
LM	3 (33.3)	8 (38.1)	0.80	2 (28.6)	2 (50.0)	0.48	0.84	0.66
LAD	4 (44.4)	7 (33.3)	0.69	0 (0.0)	1 (25.0)	0.17	0.04	0.74
LCX	2 (22.2)	2 (9.5)	0.35	2 (28.6)	1 (25.0)	0.89	0.77	0.38
RCA	0 (0.0)	1 (4.8)	0.51	0 (0.0)	0 (0.0)	NA	NA	0.67
LIMA	0 (0.0)	2 (9.5)	0.34	3 (42.9)	0 (0.0)	0.13	0.03	0.52
Venous graft								
Medications	8 (88.9)	17 (85.0)	0.78	5 (71.4)	2 (66.7)	0.88	0.38	0.44
Statin	1 (11.1)	12 (60.0)	0.01	5 (71.4)	0 (0.0)	0.04	0.01	0.05
ACE-I	9 (100.0)	20 (100.0)	NA	7 (100.0)	3 (100.0)	NA	NA	NA
ASA								

Continuous variables are expressed as the mean ± SD; categorical variables as number (%). ACE-I: angiotensin convertor enzyme inhibitor; ACS: acute coronary syndrome; ASA: acetyl salicylic acid; CABG: coronary artery bypass graft; CAD: coronary artery disease; ISR: in-stent restenosis; LAD: left anterior descending artery; LCX: left circumflex; LIMA: left internal mammary artery; LM: left main artery; MI: myocardial infarction; OCT: optical coherence tomography; RCA: right coronary artery. p: comparison within each DES generation; p*:comparison of early ISR between generations; p**: comparison of late ISR between generations.

significant ISR was included, so our results may differ from the common healing process of the stent types reported or from less pronounced in-stent proliferation not enrolled in our registry. Moreover, we support the hypothesis that the dichotomous distinction in homogeneous and heterogeneous patterns does not have a clinical correlation by itself. No data exist about the risk of clinical events correlated with a layered, as well as patchy or speckled pattern. As regards neo-atherosclerosis, relevant target in our analysis, a correlation with plaque instability and clinical events is currently a hypothesis (10–12). For instance, Kang et al. reported OCT findings indicating that stent neoatherosclerosis was frequently identified in patients with DES ISR, including TCFAs. Because the last feature was more likely to be found in patients presenting unstable angina, they supported the concept that these findings were similar to vulnerable plaques in native coronary arteries and more prone to clinical instability (32). Interestingly, in our study, TCFAs have been rarely found and, although numerically lower in second generation DES, their prevalence was similar comparing DES generations and in the overtime analysis within generations. The prognostic role of neo-atherosclerosis in ISR needs further investigations.

Neovascularization may play a role in plaque haemorrhage within de-novo lesions and influence clinical outcome (33,34). In this analysis of ISR, despite being rare, microvessels appeared significantly more common in early ISR of G1 DES. The role of neovascularization in ISR natural history is unknown.

Although our population was selected in relation to the presence of redundant intra-luminal tissue, typical of ISR, our results are consisted

Table 2
Angiographic and QCA data, analysis per lesion.

Variable	First generation (n = 44)		p	Second generation (n = 22)		p	p*	p**
	≤1 year (n = 13)	>1 year (n = 31)		≤1 year (n = 14)	>1 year (n = 8)			
Restenosis pattern								
Focal	11 (84.6)	20 (64.5)	0.28	5 (35.7)	7 (87.5)	0.02	0.02	0.40
Diffuse	2 (15.4)	11 (35.5)	0.28	9 (64.3)	1 (12.5)	0.02	0.03	0.40
QCA data								
Lesion length, mm	7.7 ± 4.5	12.2 ± 8.8	0.09	18.7 ± 14.4	7.5 ± 3.6	0.01	0.02	0.15
RD, mm	2.9 ± 0.6	3.0 ± 0.7	0.48	3.0 ± 0.6	3.0 ± 0.8	0.89	0.65	0.98
MLD, mm	1.1 ± 0.6	1.0 ± 0.5	0.75	0.8 ± 0.4	1.4 ± 0.5	<0.01	0.12	0.07
MLA, mm^2	1.2 ± 0.9	1.3 ± 1.9	0.80	0.6 ± 0.5	1.6 ± 1.2	<0.01	0.06	0.65
Diameter stenosis, %	64.0 ± 16.2	67.0 ± 15.7	0.63	71.7 ± 16.2	54.4 ± 7.1	<0.01	0.22	<0.01
Stent type								
Cypher	5 (38.5)	16 (51.6)	0.52	–	–	0.09	NA	NA
Taxus	8 (61.5)	15 (48.4)		–	–			
Xience	–	–		3 (21.4)	6 (75.0)			
Promus	–	–		2 (14.3)	0 (0.0)			
Resolute	–	–		8 (57.1)	2 (25)			
BioMatrix	–	–		1 (7.1)	0 (0.0)			
Time from previous stent to ISR	10.0 ± 2.8	37.0 ± 18.3	<0.01	8.1 ± 3.1	15.8 ± 4.0	<0.01	0.12	<0.01

Continuous variables are expressed as the mean ± SD; categorical variables as number (%). ISR: in-stent restenosis; MLA: minimal lumen area; MLD: minimal lumen diameter; QCA: quantitative coronary analysis. RD: reference diameter; p: comparison within each DES generation; p*: comparison of early ISR between generations; p**: comparison of late ISR between generations.

Table 3
Quantitative OCT analysis per cross-section with ISR > 50%.

Variable	First generation (n = 143)		p	Second generation (n = 89)		p	p*	p**
	≤1 year (n = 43)	>1 year (n = 100)		≤1 year (n = 70)	>1 year (n = 19)			
Mean stent CSA, mm^2	5.0 ± 2.1	5.1 ± 1.7	0.88	8.4 ± 3.2	4.3 ± 1.1	<0.01	<0.01	0.01
Mean lumen CSA, mm^2	1.6 ± 1.3	1.6 ± 1.2	0.86	3.2 ± 1.3	1.9 ± 0.5	<0.01	<0.01	0.08
NHI CSA, mm^2	3.5 ± 1.0	3.5 ± 0.9	0.91	5.2 ± 2.4	2.4 ± 0.7	<0.01	<0.01	<0.01
NIH area, %	72.1 ± 12.1	71.4 ± 14.9	0.79	61.1 ± 8.4	55.5 ± 5.2	<0.01	<0.01	<0.01
Restenosis length, mm	7.1 ± 11.9	5.3 ± 6.7	0.62	6.4 ± 6.4	4.7 ± 2.5	0.50	0.86	0.88

Continuous variables are expressed as the mean ± SD. CSA: cross sectional area; NIH: neo-intimal hyperplasia. p: comparison within each DES generation; p*: comparison of early ISR between generations; p**: comparison of late ISR between generations.

with previous papers reporting malapposed and uncovered struts in DES after OCT follow-up (25,26). This finding supports the concept of heterogeneity of vascular healing response after stenting, with possible co-existence of hyperplasic tissue and uncovered struts in adjacent segment (35,36), possibly due to uneven distribution of polymer and loading drug eluted, and overlapping and different deployment results in each CS.

The quantitative lesion analysis performed by both QCA and OCT showed less severe features within G2 DES, conceptually in line with the lower incidence of restenosis and TLR coming from clinical studies (13–16).

3.2. Comparison overtime within generations

This study, missing serial OCT analysis of the target restenotic lesions, does not claim to represent a reliable report of ISR pattern evolution overtime. Hence the interpretation of ISR pattern changes, based on an indirect comparison of OCT findings coming from lesions with a different follow-up, is performed aware of this limitation and is only hypothesis generating.

We found that in G1 DES the homogeneous pattern was prevalent before 1 year and even more represented afterwards. On the contrary the other patterns seemed to decrease. The heterogeneous pattern had higher prevalence in G2 both before and after 1 year, with the same absolute percentage, while neo-atherosclerosis was significantly more prevalent in the second period.

Several pathological studies confirmed that neoatherosclerotic features can be found in some restenotic lesions, often related to the time post-stent implantation (32,37). Habara et al. observed neoatherosclerotic restenosis more frequently within DES than BMS (31% vs 16%; $p < 0.001$). In the former group neo-atherosclerosis appeared to manifest earlier (420 days vs. 2160 days respectively, $p < 0.001$) (9). Available data suggest a trend toward more rapid neoatherosclerotic changes in SES, although the frequency of neo-atherosclerosis in both PES and SES was higher than that in BMS (8). The heterogeneous pattern, as well as neo-atherosclerosis, could represent delayed healing within the stented segment, correlated to individual response to each stent platform. As discussed above, this apparently more sustained inflammation within G2 DES cannot be assumed as a general rule in their healing response, neither can be directly correlated to a worse prognosis.

The mean follow-up was 29 months for G1 and 11 for G2 DES. Even if sufficient to show neo-atherosclerosis changes within DES (9), we cannot exclude that a longer time course would be needed to unmask further differences in optical ISR between groups (22). Although in BMS some authors showed that in the long term the probability of neoatherosclerotic changes rises, the same hypothesis cannot be directly applied to DES. In these devices the neoatherosclerotic phenomenon seems to start earlier but no data exist about the evolution overtime. Our data shows, at least in G1 DES, a lower prevalence of heterogeneous and neoatherosclerotic patterns in the late follow-up.

In G1 DES PSLIA prevalence decreased, whereas the opposite happened in G2 ISR, probably revealing a sustained peri-strut inflammation process. Teramoto et al. reported that PSLIA was more frequently observed with DES than BMS and that these regions were hypocellular regions, suggesting the presence of fibrinoid or proteoglycans as a consequence of delayed arterial healing (38). Their role in the possible progression of neo-atherosclerosis needs further investigation.

3.3. Limitations

The discussion has already focused on some limitations of the study, correlated to the nature of the registry enrolling selected patients with angiographically significant ISR, and the lack of serial OCT analysis. Furthermore, we want to underline that OCT has intrinsic limitations in the qualitative analysis of restenotic tissue and the differentiation of some patterns was sometimes difficult. OCT findings were not confirmed by

Table 4
OCT qualitative analysis in the entire stent.

Variable	First generation (n = 1036)		p	Second generation (n = 641)		p	p*	p**
	≤1 year (n = 309)	>1 year (n = 727)		≤1 year (n = 496)	>1 year (n = 145)			
Homogeneous	132 (42.7)	515 (70.8)	<0.01	155 (31.2)	32 (22.1)	0.04	<0.01	<0.01
Heterogeneous	117 (37.9)	161 (22.2)	<0.01	283 (57.1)	85 (58.6)	0.70	<0.01	<0.01
Layered	9 (7.7)	69 (42.9)		40 (14.1)	26 (31.7)			
Patchy	87 (75.0)	74 (46.0)		211 (7.5)	5 0(58.8)			
Speckled	21 (18.1)	18 (11.2)		32 (11.3)	9 (10.6)			
Neo-atherosclerosis	60 (19.4)	51 (7.0)	<0.01	58(11.7)	28(19.3)	0.01	<0.01	<0.01
Lipids	59 (19.1)	34 (4.7)	<0.01	49 (9.9)	26 (17.9)	0.01	<0.01	<0.01
Calcium	20 (6.5)	10 (1.4)	<0.01	7 (1.4)	4 (2.8)	0.28	<0.01	0.27
TCFA	3 (1.0)	7 (1.0)	0.99	2 (0.4)	0 (0.0)	0.98	0.32	0.61
Macrophages	3 (1.0)	6 (0.8)	0.73	3 (0.6)	0 (0.0)	0.35	0.56	0.60
Microvessels	8 (2.6)	2 (0.3)	<0.01	1 (0.2)	1 (0.7)	0.35	<0.01	0.44
PSLIA	48 (15.5)	65 (8.9)	<0.01	57 (11.5)	39 (26.9)	<0.01	0.11	<0.01
Overlapping CSs	31 (10.0)	65 (8.9)	0.56	36 (7.3)	11 (7.6)	0.86	0.19	0.75
Malapposed struts	0 (0.0)	12 (1.7)	0.08	4 (0.8)	1 (0.7)	0.89	0.11	0.65
Uncovered struts	3 (1.0)	22 (3.0)	0.04	15 (3.0)	2 (1.4)	0.39	0.08	0.41

Categorical variables are expressed as number (%). CSs: cross-sections; OCT: optical coherence tomography; PSLIA: peri-strut low intensity area. p: comparison within each DES generation; p*: comparison of early ISR between generations; p**: comparison of late ISR between generations.

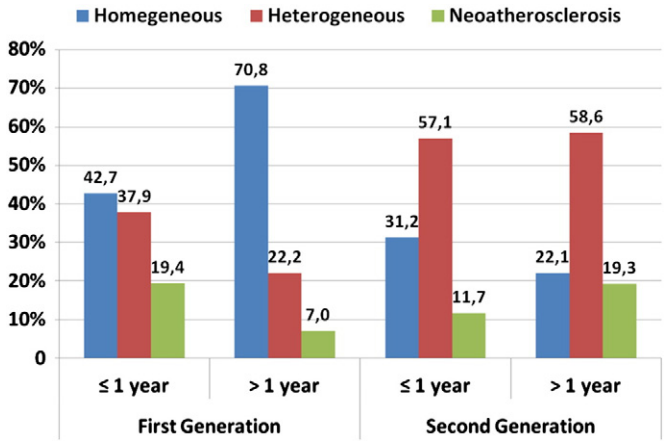

Fig. 4. Absolute prevalence of the main optical patterns of in-stent restenosis according to DES generations and early or late phase of follow-up. For statistical significance refer to Table 4.

histopathological analysis and come from observations in a relatively small number of patients.

4. Conclusions

When ISR restenosis occurs in second generation DES, the current data suggest a different time course and different morphological characteristics from first generation. Future prospective studies should evaluate the relationship between ISR morphology, time course and clinical events.

Acknowledgments

Special thanks to Mrs. Debra Dempster for the precious help in leading the research activities.

References

[1] Dangas GD, Claessen BE, Caixeta A, et al. In-stent restenosis in the drug-eluting stent era. J Am Coll Cardiol 2010;56:1897–907.
[2] Morice MC, Colombo A, Meier B, et al. Sirolimus- vs paclitaxel-eluting stents in de novo coronary artery lesions: the REALITY trial: a randomized controlled trial. JAMA 2006;295:895–904.
[3] Yabushita H, Bouma BE, Houser SL, et al. Characterization of human atherosclerosis by optical coherence tomography. Circulation 2002;106:1640–5.
[4] Brezinski ME, Tearney GJ, Bouma BE, et al. Optical coherence tomography for optical biopsy. Properties and demonstration of vascular pathology. Circulation 1996;93:1206–13.
[5] Prati F, Regar E, Mintz GS, et al. Expert review document on methodology, terminology, and clinical applications of optical coherence tomography: physical principles, methodology of image acquisition, and clinical application for assessment of coronary arteries and atherosclerosis. Eur Heart J 2010;31:401–15.
[6] Gonzalo N, Serruys PW, Okamura T, et al. Optical coherence tomography patterns of stent restenosis. Am Heart J 2009;158:284–93.
[7] Bossi I, Klersy C, Black AJ, et al. In-stent restenosis: long-term outcome and predictors of subsequent target lesion revascularization after repeat balloon angioplasty. J Am Coll Cardiol 2000;35:1569–76.
[8] Nakazawa G, Otsuka F, Nakano M, et al. The pathology of neoatherosclerosis in human coronary implants bare-metal and drug-eluting stents. J Am Coll Cardiol 2011;57:1314–22.
[9] Habara M, Terashima M, Nasu K, et al. Difference of tissue characteristics between early and very late restenosis lesions after bare-metal stent implantation: an optical coherence tomography study. Circ Cardiovasc Interv 2011;4:232–8.
[10] Kolodgie FD, Burke AP, Farb A, et al. The thin-cap fibroatheroma: a type of vulnerable plaque: the major precursor lesion to acute coronary syndromes. Curr Opin Cardiol 2001;16:285–92.
[11] Falk E, Nakano M, Bentzon JF, Finn AV, Virmani R. Update on acute coronary syndromes: the pathologists' view. Eur Heart J 2013;34:719–28.
[12] Saia F, Schaar J, Regar E, et al. Clinical imaging of the vulnerable plaque in the coronary arteries: new intracoronary diagnostic methods. J Cardiovasc Med (Hagerstown) 2006;7:21–8.
[13] Leon MB, Nikolsky E, Cutlip DE, et al. Improved late clinical safety with zotarolimus-eluting stents compared with paclitaxel-eluting stents in patients with de novo coronary lesions: 3-year follow-up from the ENDEAVOR IV (Randomized Comparison of Zotarolimus- and Paclitaxel-Eluting Stents in Patients With Coronary Artery Disease) trial. JACC Cardiovasc Interv 2010;3:1043–50.
[14] Stefanini GG, Kalesan B, Serruys PW, et al. Long-term clinical outcomes of biodegradable polymer biolimus-eluting stents versus durable polymer sirolimus-eluting stents in patients with coronary artery disease (LEADERS): 4 year follow-up of a randomised non-inferiority trial. Lancet 2011;378:1940–8.
[15] Byrne RA, Kastrati A, Massberg S, et al. Biodegradable polymer versus permanent polymer drug-eluting stents and everolimus- versus sirolimus-eluting stents in patients with coronary artery disease: 3-year outcomes from a randomized clinical trial. J Am Coll Cardiol 2011;58:1325–31.
[16] Serruys PW, Silber S, Garg S, et al. Comparison of zotarolimus-eluting and everolimus-eluting coronary stents. N Engl J Med 2010;363:136–46.
[17] Stefanini GG, Serruys PW, Silber S, et al. The impact of patient and lesion complexity on clinical and angiographic outcomes after revascularization with zotarolimus- and everolimus-eluting stents: a substudy of the RESOLUTE All Comers Trial (a randomized comparison of a zotarolimus-eluting stent with an everolimus-eluting stent for percutaneous coronary intervention). J Am Coll Cardiol 2011;57:2221–32.
[18] Windecker S, Serruys PW, Wandel S, et al. Biolimus-eluting stent with biodegradable polymer versus sirolimus-eluting stent with durable polymer for coronary revascularisation (LEADERS): a randomised non-inferiority trial. Lancet 2008;372:1163–73.
[19] Mehran R, Dangas G, Abizaid AS, et al. Angiographic patterns of in-stent restenosis: classification and implications for long-term outcome. Circulation 1999;100:1872–8.
[20] Goto K, Takebayashi H, Kihara Y, et al. Appearance of neointima according to stent type and restenotic phase: analysis by optical coherence tomography. EuroIntervention 2013;9:601–7.
[21] Habara M, Terashima M, Nasu K, et al. Morphological differences of tissue characteristics between early, late, and very late restenosis lesions after first generation drug-eluting stent implantation: an optical coherence tomography study. Eur Heart J Cardiovasc Imaging 2013;14:276–84.
[22] Takano M, Yamamoto M, Inami S, et al. Appearance of lipid-laden intima and neovascularization after implantation of bare-metal stents extended late-phase observation by intracoronary optical coherence tomography. J Am Coll Cardiol 2009;55:26–32.
[23] Tearney GJ, Yabushita H, Houser SL, et al. Quantification of macrophage content in atherosclerotic plaques by optical coherence tomography. Circulation 2003;107:113–9.
[24] Otake H, Shite J, Ikeno F, et al. Evaluation of the peri-strut low intensity area following sirolimus- and paclitaxel-eluting stents implantation: insights from an optical coherence tomography study in humans. Int J Cardiol 2012;157:38–42.
[25] Barlis P, Dimopoulos K, Tanigawa J, et al. Quantitative analysis of intracoronary optical coherence tomography measurements of stent strut apposition and tissue coverage. Int J Cardiol 2010;141:151–6.
[26] Takano M, Yamamoto M, Inami S, et al. Long-term follow-up evaluation after sirolimus-eluting stent implantation by optical coherence tomography: do uncovered struts persist? J Am Coll Cardiol 2008;51:968–9.
[27] Cassese S, Byrne RA, Tada T, et al. Incidence and predictors of restenosis after coronary stenting in 10 004 patients with surveillance angiography. Heart 2014;100:153–9.
[28] Chen MS, John JM, Chew DP, Lee DS, Ellis SG, Bhatt DL. Bare metal stent restenosis is not a benign clinical entity. Am Heart J 2006;151:1260–4.
[29] Farb A, Shroff S, John M, Sweet W, Virmani R. Late arterial responses (6 and 12 months) after (32)P beta-emitting stent placement: sustained intimal suppression with incomplete healing. Circulation 2001;103:1912–9.
[30] Nagai H, Ishibashi-Ueda H, Fujii K. Histology of highly echolucent regions in optical coherence tomography images from two patients with sirolimus-eluting stent restenosis. Catheter Cardiovasc Interv 2010;75:961–3.
[31] Chung IM, Gold HK, Schwartz SM, Ikari Y, Reidy MA, Wight TN. Enhanced extracellular matrix accumulation in restenosis of coronary arteries after stent deployment. J Am Coll Cardiol 2002;40:2072–81.
[32] Kang SJ, Mintz GS, Akasaka T, et al. Optical coherence tomographic analysis of in-stent neoatherosclerosis after drug-eluting stent implantation. Circulation 2011;123:2954–63.
[33] Virmani R, Kolodgie FD, Burke AP, et al. Atherosclerotic plaque progression and vulnerability to rupture: angiogenesis as a source of intraplaque hemorrhage. Arterioscler Thromb Vasc Biol 2005;25:2054–61.
[34] Moreno PR, Purushothaman KR, Sirol M, Levy AP, Fuster V. Neovascularization in human atherosclerosis. Circulation 2006;113:2245–52.
[35] Otsuka F, Nakano M, Ladich E, Kolodgie FD, Virmani R. Pathologic etiologies of late and very late stent thrombosis following first-generation drug-eluting stent placement. Thrombosis 2012;2012:608593.
[36] Finn AV, Joner M, Nakazawa G, et al. Pathological correlates of late drug-eluting stent thrombosis: strut coverage as a marker of endothelialization. Circulation 2007;115:2435–41.
[37] Nakazawa G, Vorpahl M, Finn AV, Narula J, Virmani R. One step forward and two steps back with drug-eluting-stents: from preventing restenosis to causing late thrombosis and nouveau atherosclerosis. JACC Cardiovasc Imaging 2009;2:625–8.
[38] Teramoto T, Ikeno F, Otake H, et al. Intriguing peri-strut low-intensity area detected by optical coherence tomography after coronary stent deployment. Circ J 2010;74:1257–9.